Photothermally-induced disordered patterns of corneal collagen revealed by SHG imaging

Paolo Matteini,[1] Fulvio Ratto,[1] Francesca Rossi,[1] Riccardo Cicchi,[2] Chiara Stringari,[2] Dimitrios Kapsokalyvas,[2] Francesco S. Pavone,[2] and Roberto Pini,[1,*]

[1]Istituto di Fisica Applicata "Nello Carrara", Consiglio Nazionale delle Ricerche, Via Madonna del Piano 10, Sesto Fiorentino, I-50019, Italy

[2]LENS, European Laboratory for Non-Linear Spectroscopy, Via Nello Carrara 1, Sesto Fiorentino, I-50019, Italy

[*]Corresponding author: R.Pini@ifac.cnr.it

Abstract: The loss of organization of the corneal collagen lattice induced by photothermal effects was analyzed by using second-harmonic generation (SHG) imaging. Porcine cornea samples were treated with low-power laser irradiation in order to get localized areas of tissue disorganization. The disorder induced within the irradiated area of corneal stroma was quantified by means of Discrete Fourier Transform, auto-correlation and entropy analyses of the SHG images. Polarization modulated SHG measurements allowed to probe the changes in the structural anisotropy of sub-micron hierarchical levels of the stromal collagen. Our results emphasize the great potential of the SHG imaging to detect subtle modifications in the collagen assembly. The proposed analytical methods may be used to track several genetic, pathologic, accidental or surgical-induced disorder states of biological tissues.

OCIS codes: (180.0180) Microscopy; (180.4315) Nonlinear microscopy; (350.5340) Photothermal effects; (170.3880) Medical and biomedical imaging.

References and links

1. W. R. Zipfel, R. M. Williams, R. Christie, A. Y. Nikitin, B. T. Hyman, and W. W. Webb, "Live tissue intrinsic emission microscopy using multiphoton-excited native fluorescence and second harmonic generation," Proc. Natl. Acad. Sci. USA **100**, 7075-7080 (2003).
2. P. J. Campagnola and L. M. Loew, "Second-harmonic imaging microscopy for visualizing biomolecular arrays in cells, tissues and organisms.," Nat. Biotechnol. **21**, 1356-1360 (2003).
3. E. Brown, T. McKee, E. dI Tomaso, A. Pluen, B. Seed, Y. Boucher, and R. K. Jain, "Dynamic imaging of collagen and its modulation in tumors in vivo using second-harmonic generation," Nat. Med. **9**, 796-800 (2003).
4. R. Cicchi, D. Massi, S. Sestini, P. Carli, V. De Giorgi, T. Lotti, and F. S. Pavone, "Multidimensional non-linear laser imaging of basal cell carcinoma," Opt. Express **15**, 10135-10148 (2007).
5. O. Nadiarnykh, S. Plotnikov, W. A. Mohler, I. Kalajzic, D. Redford-Badwal, and P. J. Campagnola, "Second harmonic generation imaging microscopy studies of osteogenesis imperfecta," J. Biomed. Opt. **12**, 051805 (2007).
6. S. Roth and I. Freund, "Second harmonic generation in collagen," J. Chem. Phys. **70**, 1637-1643 (1979).
7. P. Stoller, K. M. Reiser, P. M. Celliers, and A. M. Rubenchik, "Polarization-modulated second harmonic generation in collagen," Biophys. J. **82**, 3330-3342 (2002).
8. K. M. Reiser, C. Bratton, D. R. Yankelevich, A. Knoesen, I. Rocha-Mendoza, and J. Lotz, "Quantitative analysis of structural disorder in intervertebral disks using second harmonic generation imaging: comparison with morphometric analysis," J. Biomed. Opt. **12**, 064019 (2007).
9. R. Lacomb, O. Nadiarnykh, and P. J. Campagnola, "Quantitative second harmonic generation imaging of the diseased state osteogenesis imperfecta: experiment and simulation," Biophys. J. **94**, 4504-4014 (2008).
10. Y. Komai and T. Ushiki, "The three-dimensional organization of collagen fibrils in the human cornea and sclera," Invest. Ophtalmol. Visual. Sci. **32**, 2244-2258 (1991).
11. P. Matteini, F. Rossi, L. Menabuoni, and R. Pini, "Microscopic characterization of collagen modifications induced by low-temperature diode-laser welding of corneal tissue," Lasers Surg. Med. **39**, 597-604 (2007).
12. F. Rossi, R. Pini, and L. Menabuoni, "Experimental and model analysis on the temperature dynamics during diode laser welding of the cornea," J. Biomed. Opt. **12**, 014031 (2007).
13. S. J. Lin, C. Y. Hsiao, Y. Sun, W. Lo, W. C. Lin, G. J. Jan, S. H. Jee, and C. Y. Dong, "Monitoring the thermally induced structural transitions of collagen by use of second-harmonic generation microscopy," Opt. Lett. **30**, 622-624 (2005)

#103227 - $15.00 USD Received 24 Oct 2008; revised 26 Nov 2008; accepted 27 Nov 2008; published 13 Mar 2009

14. T. Theodossiou, G. S. Rapti, V. Hovhannisyan, E. Georgiou, K. Politopoulos, and D. Yova, "Thermally induced irreversible conformational changes in collagen probed by optical second harmonic generation and laser-induced fluorescence," Lasers Med. Sci. **17**, 34-41 (2002)
15. F. Rossi, R. Pini, L. Menabuoni, R. Mencucci, U. Menchini, S. Ambrosini, and G. Vannelli, "Experimental study on the healing process following laser welding of the cornea," J. Biomed. Opt. **10**, 024004 (2005).
16. R. Cicchi, S. Sestini, V. De Giorgi, D. Massi, T. Lotti, and F. S. Pavone, "Non-linear laser imaging of skin lesions," J. Biophotonics **1**, 62-73 (2008).
17. F. Rossi, P. Matteini, I. Bruno, P. Nesi, and R. Pini, "Monitoring thermally-induced phase-transitions in porcine cornea with the use of fluorescence micro-imaging analysis," Opt. Express **15**, 11178-11184 (2007).
18. R. Holota and S. Němeček, *Applied Electronics*, J. Pinker, ed., (University of West Bohemia, Pilsen, 2002).
19. J. Kuczyński and P. Mikołajczak, "Information theory based medical images processing," Opto-Electron. Rev. **11**, 253-259 (2003).
20. R. Gauderon, P. B. Lukins, and C. J. Sheppard, "Optimization of second-harmonic generation microscopy," Micron **32**, 691-700 (2001).
21. M. Han, G. Giese, and J. F. Bille, "Second harmonic generation imaging of collagen fibrils in cornea and sclera," Opt. Express **13**, 5791-5797 (2005).
22. S. W. Chu, S. Y. Chen, G. W. Chern, T. H. Tsai, Y. C. Chen, B. L. Lin, and C. K. Sun, "Studies of $\chi^{(2)}$/ $\chi^{(3)}$ tensors in submicron-scaled bio-tissues by polarization harmonics optical microscopy," Biophys. J **86**, 3914-3922 (2004).
23. F. Tiaho, G. Recher, and D. Rouède, "Estimation of helical angles of myosin and collagen by second harmonic generation imaging microscopy," Opt. Express **15**, 12286-12295 (2007).
24. P. Stoller, B. M. Kim, A. M. Rubenchik, K. M. Reiser, and L. B. Da Silva, "Polarization-dependent optical second-harmonic imaging of a rat-tail tendon," J. Biomed. Opt. **7**, 205-214 (2002).
25. C. K. Chou, W. L. Chen, P. T. Fwu, S. J. Lin, H. S. Lee, and C. Y. Dong, "Polarization ellipticity compensation in polarization second-harmonic generation microscopy without specimen rotation," J. Biomed. Opt. **13**, 014005 (2008).

1. Introduction

Second harmonic generation (SHG) imaging is an emerging microscopy technique, which is particularly well suited to analyze connective tissues due to the significant second order nonlinear susceptibility of collagen [1,2]. This confers high contrast and specificity to the SHG images. Moreover the intrinsically noninvasive nature of this technique further enhances its potential to become a clinical tool to perform *ex vivo* biopsies or *in vivo* imaging. SHG signals have been used to discriminate cancerous tissue [3,4] and genetic disorders [5], which are related to altered content and assembly of the collagen matrix resulting in a modulation of the SHG intensity. In addition, SHG microscopy holds great potential in differentiating normal and abnormal structures by using a polarization-modulation approach, which exploits the coherent nature of the second harmonic signal [6-9]. Overall SHG imaging is presently considered a powerful technique to investigate tissue structure and organization, and may become a noninvasive complement to traditional structural methods such as electron microscopy, X-ray diffraction and histological analysis.

The corneal stroma displays a very regular assembly of collagen fibrils (~30 nm in size) which are arranged parallel to each other into lamellar domains (i.e. 0.5-2.5 μm thick planar structures running parallel to the corneal surface) [10]. The highly ordered nature of this tissue makes it a convenient model to study disorganization events of the normal connective matrix. In our study, we used SHG imaging to quantify the photothermally-induced modifications in the fibrillar collagen assembly of laser-treated porcine corneas. The morphological and thermodynamic properties of this model have been thoroughly characterized in the context of early experiences of laser welding [11,12]. When the corneal stroma undergoes low-power continuous wave diode-laser treatment, a controlled thermal effect can be induced within the irradiated volume. The result is a mild perturbation of the regular fibrillar arrangement, while uncontrolled denaturation of collagen is avoided [11]. Moreover, the extent of lattice disorder decreases smoothly and progressively with the distance from the center of the irradiated area. Such a model enables the study and comparison of different disorganization patterns on the same tissue sample.

Recently proposed methods to study heat-induced structural changes of collagen-based lattices rely on following the variation of the SHG intensity while rising the temperature [13, 14]. However, an approach based uniquely on an estimate of the loss of signal intensity may

#103227 - $15.00 USD Received 24 Oct 2008; revised 26 Nov 2008; accepted 27 Nov 2008; published 13 Mar 2009

be inadequate to accurately characterize the collagen modifications at different levels of structural organization. In this paper we propose a more refined method to correlate the modulation of the SHG signal with the disorganization of the corneal collagen. We first adopted an image analysis approach to quantify the different structural patterns of lamellar assembly generated by the laser irradiation. Then we extracted maps of the local orientation of the fibrillar lattice and investigated the typical distance over which the regular sub-lamellar arrangement is preserved. Finally, we compared the second-harmonic polarization profiles from non-irradiated and irradiated areas, in order to highlight differences in the interfibrillar arrangement at the smallest resolvable length scale of our microscope. A parallel transmission electron microscopy (TEM) analysis was performed to further support the SHG data.

2. Materials and methods

2.1 Sample treatment

Ten porcine eyes were enucleated and kept in a humid environment until the time of experiments, typically 12 h after their extraction. The cornea was explanted and sliced in 1-mm-thick cross-sections with a razor blade. In order to induce a controlled temperature rise in the samples, each cornea was treated under usual conditions for the low-power diode-laser welding procedure [15]. In doing this, one side of the slice was stained with a water solution (10 % w/w) of a chromophore (Indocyanine Green, ICG). The stain was then washed out after 2 min, in order to remove the excess of chromophore not absorbed by the tissue. ICG is an effective optical absorber of laser radiation emitted at 810 nm, and so it can mediate a localized and well-controlled photothermal effect within the tissue [12]. The laser device we used was an AlGaAs diode (Mod. Weld 800, El.En., Italy), equipped with an optical fiber of 300 μm-core diameter (NA 0.24). The fiber tip, which was kept at a constant distance of 1 mm from the surface of the slide, delivered to the sample a power of 40 mW (8.3 W/cm^2) for an overall time irradiation of 2 s. These parameters allowed to confine the photothermal effect within a ~400 μm-radius spot (see Fig. 1), inducing a gradient of disorganization in the corneal collagen from the centre to the periphery and beyond the irradiated area. After the treatment, the samples were stored in formalin until the SHG images were acquired.

Laser-treated cornea slices were then processed for TEM measurements. In brief, they were fixed in glutaraldehyde and cut into 1 mm^2 samples including the laser-treated portion. The samples were postfixed in osmium tetroxide and, after sequential dehydration, were infiltrated in Epon resin. Ultra-thin sections were cut and stained with uranyl acetate and lead citrate, and examined with an electron microscope (Philips CM-12, Philips Industries, Eindhoven, The Nederlands). Micrographs of representative fields of control and irradiated regions were taken from each specimen.

#103227 - $15.00 USD Received 24 Oct 2008; revised 26 Nov 2008; accepted 27 Nov 2008; published 13 Mar 2009

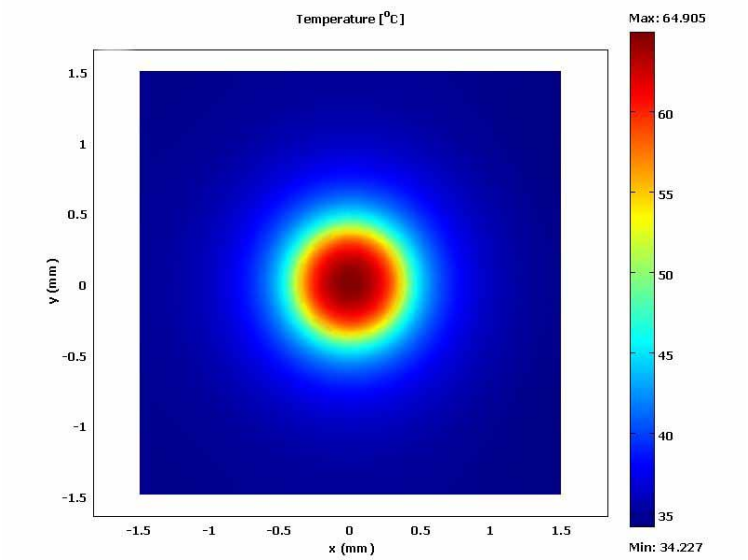

Fig. 1. Temperature development within a ~400 μm-radius spot area of a corneal slice subjected to diode laser irradiation. The data are the result of a 3D model (obtained with the software Comsol Multiphysics 3.4 (Comsol AB, Sweden)), based on the solution of the bio-heat equations, which describes the photothermal effects induced by the diode laser irradiation (40 mW power output, 2 s irradiation time) inside the tissue [12].

2.2 SHG microscopy system

The experimental setup consisted of a modified inverted microscope (Nikon TE300, Nikon Instruments, Tokyo, Japan). Detailed descriptions of the SHG microscope have been given previously [16]. Briefly, the excitation was accomplished by a mode-locked Ti:Sapphire laser emitting 120-fs width pulses at a 90-MHz repetition rate, a wavelength of 880 nm and an average power at the sample between 1 and 10 mW, depending on the depth of recording. The beam was focused onto the sample by a 50× 0.95 NA oil immersion objective (Nikon Plan-Apo, 0.35 mm WD, Nikon Instruments, Japan), and collected using a 60× 1.00 NA long working distance water immersion objective (Nikon Plan-Fluor, 2 mm WD, Nikon Instruments, Japan). A quarter-wave plate and a linear polarizer are placed immediately before the back focal plane of the focusing objective. The broad band (690-1200 nm) quarter-wave plate is mounted on a micromanipulator to obtain a circularly polarized light (with ellipticity equal to 1 within an error of 4%). A variable linear polarization of the exciting beam is accomplished through a linear polarizer mounted on a motorized rotating stage in order to rotate the polarization angle of the incident electric field without movement of the biological specimen. The SHG signal was isolated from the fundamental and any fluorescence by a 440 ± 5 nm band-pass filter (Z440BP, Chroma Technology Corporation, Rockingham, VT, US). For all imaging not involving the polarization analysis, the laser excitation was circularly polarized. The pixel dwell time was set to 5 μs/pixel. The scanning time was approximately 0.8 s for a 500×500 pixels image. Image areas of 60×60 μm^2 (0.12 μm/pixel), 500×500 pixels were considered, unless otherwise specified, for the analysis reported below.

2.3 Image analysis of lamellar anisotropy

The analysis of the circularly polarized SHG corneal images was performed by means of two image processing techniques: the two-dimensional Discrete Fourier Transform (2D DFT) and the image entropy [17]. The processing algorithms were developed in the Matlab and IGOR Pro platforms (Matlab 7.0, the Mathworks, Natick, MA; IGOR Pro 4.07, WaveMetrics Inc. Lake Oswego, OR).

#103227 - $15.00 USD Received 24 Oct 2008; revised 26 Nov 2008; accepted 27 Nov 2008; published 13 Mar 2009

The frequency distribution in a Fourier-transformed image can be analyzed to retrieve the pattern of image line directions, so as to characterize the geometry of the image texture [18]. Thus, the 2D DFT of each image was computed and the logarithm of the absolute value of the calculated DFT was displayed. Next, the DFT magnitude was thresholded to levels 0 or 1. The degree of DFT deformation was quantitatively calculated by fitting the result with an ellipse and by calculating the ratio between its short and long axes, i.e. its aspect ratio (AR).

The entropy is a statistical index widely used in the field of information theory to express the information content of a message. The entropy of the image intensity can be used to characterize its texture randomness [19]. Images were processed by applying the edge function based on Canny filter, to extract the spatial distribution of the collagen matrix. The calculation of the entropy E of an image with *n* grey levels was obtained by Eq. (1):

$$E = -\sum_{i=1}^{n} p(g_i)\log(p(g_i)) \tag{1}$$

where $p(g_i)$ is the histogram value of the *i*-th grey level g_i. We defined a Disorganization Parameter (DP) as the inverse of *E* [17], and used it for subsequent analysis (growing DP values correspond to an increasingly disordered content of an image texture). Finally, AR and DP values, calculated for selected regions taken at different distances from the middle of the laser-irradiated area, were compared.

2.4 Polarization analysis of sub-lamellar anisotropy

To assess the extent of the modification of the sub-lamellar assembly of the collagen matrix upon laser treatment, we investigated the dependence of the SHG signal on the polarization angle of the excitation light. We acquired series of images at different polarization angles (with steps of 10°) for selected control and irradiated areas of the laser-treated tissue. A twofold approach for the analysis of the polarization data was followed.

2.4.1 Analysis of the sub-lamellar arrangement

The polarization profile of the SHG intensity acquired from individual pixels exhibits a typical pattern of minima and maxima (see e.g. the experimental data (♦) in Fig. 2). As a rule of thumb, the minima are obtained when the polarization of the excitation light lies orthogonal to the principal axis of the collagen fibrils [8]. The identification of these minima allows for the construction of laterally resolved maps of the angles α which define the local mean orientation of the collagen fibrils within each pixel. The lateral resolution of these maps is about the size of the focal volume (i.e. about 400 nm as estimated by the Rayleigh criterion [20], with a 0.95 NA objective and λ = 880 nm). These maps allowed us to investigate the lateral correlation between the mutual orientations of the collagen fibrils through an immediate auto-correlation analysis. The auto-correlation matrices:

$$C(d_x, d_y) \equiv \frac{\sum_{i,j} \alpha(i + d_x, j + d_y)\alpha(i, j)}{\sum_{i,j} \alpha(i, j)^2}, \tag{2}$$

where the discrete variables d_x and d_y are the length along the horizontal and vertical directions, were computed from the data at different distances from the irradiated area, and then fitted to an isotropic exponential decay:

$$C(d_x, d_y) \equiv 10^{-\frac{\sqrt{d_x^2 + d_y^2}}{L}}, \tag{3}$$

in order to obtain a quantitative estimate of a correlation length *L*. The latter is taken to represent the typical distance over which the regular sub-lamellar arrangement is preserved.

#103227 - $15.00 USD Received 24 Oct 2008; revised 26 Nov 2008; accepted 27 Nov 2008; published 13 Mar 2009

2.4.2 Analysis of the interfibrillar alignment at the sub-micron scale

To investigate the laser-induced changes in the interfibrillar alignment, we analyzed polarization profiles from individual points (0.5 μm size) from treated and untreated areas of the corneal stroma. The appearance of the average profiles (average over 1000 randomly selected profiles per kind of area) provides qualitative insight of the modifications involved in the photothermal process.

Then we treat the polarization profiles in analogy to a time domain signal, and pursue a quantitative estimate of the main differences between the data from treated and untreated areas over a frequency domain, i.e. by an FFT analysis. In practice, a typical polarization profile can be decomposed into the sum of three main contributions, which are: 1) a zero frequency level, 2) a modulation signal found at low frequencies, 3) a supposedly white noise, which dominates at high frequencies (see the example in Fig. 2). In the analysis below we set a threshold for the upper frequency of the modulation signal at 1/60°, i.e. any maxima and minima narrower than three data points is treated as noise fluctuations.

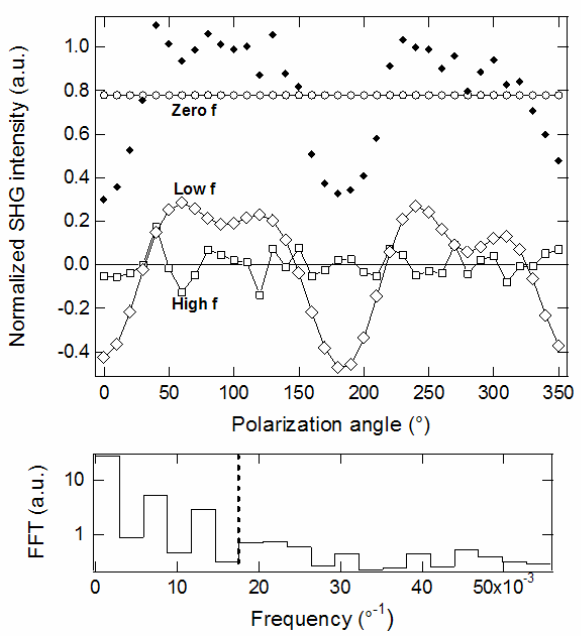

Fig. 2. FFT of a polarization-modulated SHG profile. Upper: frequency (f) decomposition of the experimental data (♦) into zero (○), low (◊) and high (□) frequency contributions. Lower: frequency distribution (log scale).

The component at zero frequency simply represents the polarization-averaged SHG intensity. The components at low frequencies account for the main modulation of the signal as due to the local orientation of the fibrillar lattice. Conversely the components at high frequencies are interpreted as pure noise fluctuations. With these assumptions, we computed the FFT of the SHG intensities and calculated an effective Modulation Parameter (*MP*) as the average amplitude of the FFT modulus at low frequencies $\langle I \rangle_{LF}$ minus the noise level $\langle I \rangle_{HF}$ (extrapolated from the average amplitude of the FFT modulus at high frequencies) and normalized by the intensity at zero frequency I_0:

$$MP = \frac{\langle I \rangle_{LF} - \langle I \rangle_{HF}}{I_0}. \quad (4)$$

#103227 - $15.00 USD Received 24 Oct 2008; revised 26 Nov 2008; accepted 27 Nov 2008; published 13 Mar 2009

The values of this parameter may give an indication of the extent of the alignment of the fibrils within the single point. We calculated the *MP* from individual polarization profiles and compared their average values from treated and untreated areas (average over 1000 profiles per kind of area).

3. Results and discussion

The circularly polarized SHG images of the corneal stroma (Fig. 3) revealed ~ 0.5 μm thick fiber-like structures, which actually consisted of many collagen fibrils, organized in lamellar domains, and which were previously referred to as fibrillar bundles [21]. The size of these structures is comparable with the minimum resolvable distance for our microscope (~ 400 nm, i.e. the size of the focal volume given by the Rayleigh criterion, see Sec. 2.4.1).

Figure 4 displays an example of a stack of four images taken at different distances from the center of a ~ 400 μm-radius laser-irradiated spot area. These four regions of interest (ROIs, 60×60 μm^2 each) well represent the progressive collagen disorganization. At the exterior of the spot (ROI (a)) a parallel arrangement of waved lamellar planes is clearly visible. Moving towards the center of the laser-treated area (ROIs (b) - (d)), the lamellar arrangement is progressively lost and a dense packing of increasingly disordered collagen bundles appears. Correspondingly, the 2D DFT diagrams transform from elliptical to circular shapes, which indicates a transition towards random patterns. The increase of the corresponding AR is evident when moving from the periphery to the center of the spot as shown in Fig. 5(a). The wavy behavior of the collagen lamellae is interpreted as the reason why the AR values never go below 0.6, even in control untreated regions. The DP also increases when moving toward regions of higher tissue randomization (Fig. 5(b)). It is noteworthy to underline the higher capacity of the AR to reveal transitions from normal or rather-structured (ROIs (a) and (b)) to more disorganized patterns (ROIs (c) and (d)). In contrast the DP parameter is more sensitive to discriminate between patterns of higher disorder (compare ROIs (c) and (d)).

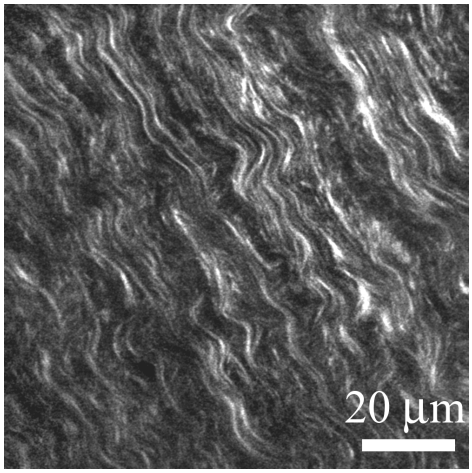

Fig. 3. SHG image of an intact porcine corneal stroma.

#103227 - $15.00 USD Received 24 Oct 2008; revised 26 Nov 2008; accepted 27 Nov 2008; published 13 Mar 2009

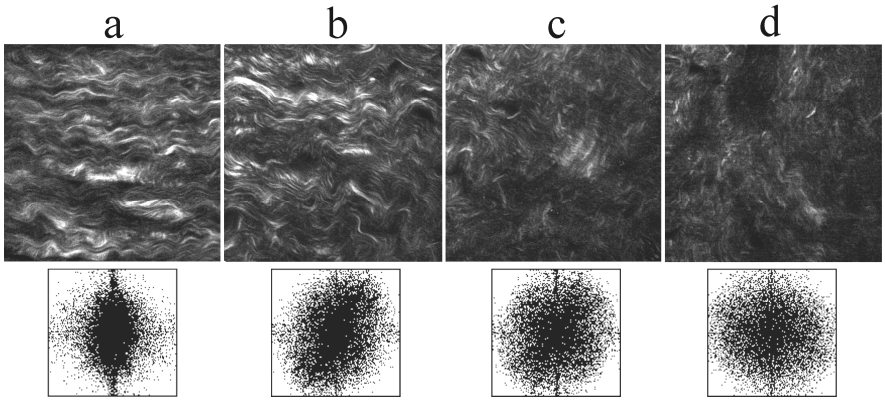

Fig. 4. Stack of SHG images (60×60 μm^2 ROIs) taken from the periphery to the center of a laser-irradiated spot area. The radial distance of the ROIs from the center of the irradiation spot area are 600 μm (a); 400 μm (b); 200 μm (c); 0 μm (d). The DFT diagram of each ROI is also shown in the lower panels.

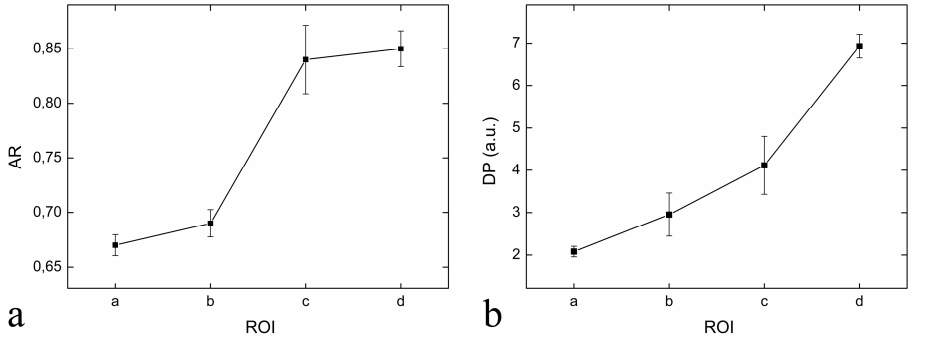

Fig. 5. Plot of the mean value (± SD) of: (a) the Aspect Ratio (AR) of the ellipse approximating the DFT magnitude and (b) the Disorganization Parameter (DP) of ROIs at different distances from the irradiated spot area, as represented in Fig. 4. Each data point is the average over values from different regions of the same sample.

In order to gain further insight into the induced stromal arrangement, we carried out an analysis of the sub-lamellar assembly. Although the resolution of our SHG microscope is not enough to detect individual corneal fibrils (the fibrillar size is ~30 nm), it may still be effective to investigate the mutual organization of fibrils within each lamella (of the order of the resolution of our set-up). Indeed the acquisition and analysis of polarization-modulated SHG signals has been shown to provide a very fine description of the local matrix anisotropy [7,22-25].

As a first step, by the analysis of the minima in the polarization profiles, we extracted the local orientation of the fibrillar lattice from representative areas (8×8 μm^2) (as depicted in Figs. 6(a), 6(d) and 6(g)), taken at three different distances from the periphery toward the center of a laser-irradiated area. We built two dimensional maps of the values of α, which denotes the local mean orientation of the collagen fibrils within each pixel (see Figs. 6(b), 6(e) and 6(h)). Then we calculated the lateral correlation among these orientations, which represents the typical distance over which the regular sub-lamellar arrangement is preserved. Correlation lengths of around 2.9, 1.5 and 0.4 microns were found for the three areas examined (Figs. 6(c), 6(f) and 6(i)). The calculated correlation length for the control area is

#103227 - $15.00 USD Received 24 Oct 2008; revised 26 Nov 2008; accepted 27 Nov 2008; published 13 Mar 2009

compatible with the mean size of the individual stromal lamellae (typically from 0.5 to 2.5 μm thick, see e.g. [10]). On the other hand, the value associated to the center of the spot area is very close to the resolution of our microscope (see Sec. 2.4.1), as expected in a highly disordered matrix. These results are in agreement with the aforementioned observations on a progressive loss of the lamellar domains when moving from the periphery toward the center of a laser-irradiated spot area.

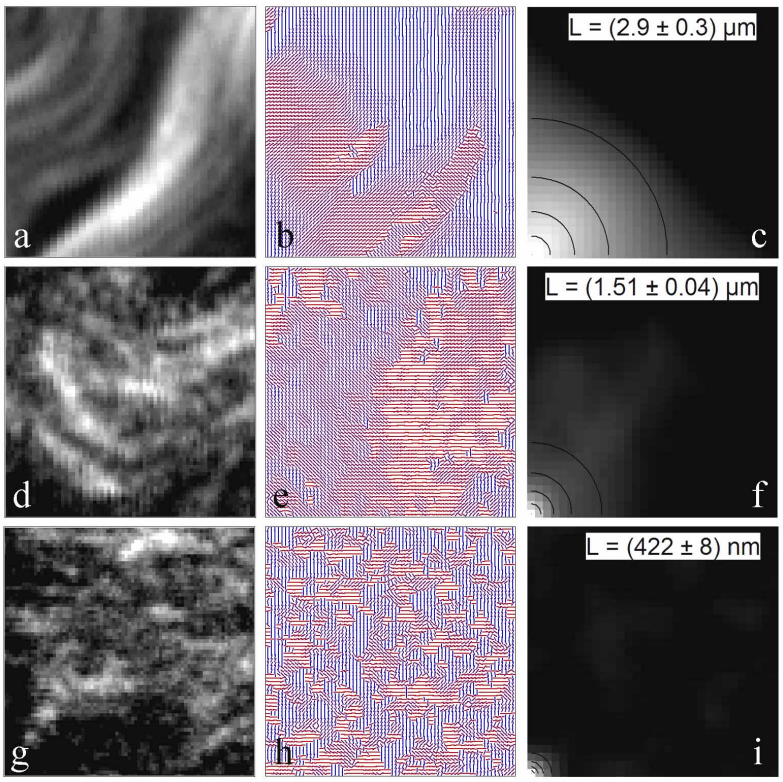

Fig. 6. Analysis of the sub-lamellar arrangement. SHG images (8×8 μm^2) (a,d,g), maps of the orientations of the collagen fibrils (b,e,h), and auto-correlation matrices (c,f,i) taken at a distance of 600 μm (a,b,c); 300 μm (d,e,f); 0 μm (g,h,i) from the center of the laser-irradiated spot area. *L* is taken to represent the typical distance over which the regular sub-lamellar arrangement is preserved.

The final step of our analysis was the investigation of the loss of anisotropy at sub-micron structural levels of the stromal architecture (i.e. about the minimum resolvable distance of our microscope). To this aim, we extracted and averaged the polarization profiles from single points (0.5 μm size, n = 1000) taken randomly from untreated (Fig. 7(a)) and irradiated (Fig. 7(d)) areas, as reported in Figs. 7(b) and 7(e) respectively. The random procedure is intended to evenly represent all the possible mean orientations of the collagen fibrils in the two samples (which may in general exhibit an out-of-plane component). In addition we performed a TEM analysis to validate our polarization-modulated SHG results on the sub-micron structure of our samples (see Figs. 7(c) and 7(f)). The SHG profile obtained from the control area exhibits a significant modulation which is believed to originate from a highly ordered interfibrillar arrangement, in agreement with the TEM analysis. Indeed the corresponding TEM micrographs display the alternation of regular lamellar domains, composed of well-aligned collagen fibrils. By contrast, the SHG-profile relative to the treated area is partially degraded. This result may be consistent with either of two different dynamics, i.e. the loss of regular

#103227 - $15.00 USD Received 24 Oct 2008; revised 26 Nov 2008; accepted 27 Nov 2008; published 13 Mar 2009

alignment of the collagen fibrils already over the length scale of the available resolution, or the loss of integrity of the collagen fibrils (i.e. a degradation of the SHG-generators due to the thermal denaturation of the collagen molecules). The TEM analysis revealed the coexistence of sub-lamellar groups of differently oriented and interwoven fibrils, which however preserve their individual integrity and never display the fingerprints of denaturation (fibril swelling which increases the fibrillar diameter, and loss of edge sharpness). Thus, we deduce that the fibrillar bundles observed in the SHG images of laser-irradiated areas may probably represent packets of native collagen fibrils, which still keep an average preferential orientation against an increasing degree of local disorder. This mild perturbation of the regular fibrillar arrangement is fully consistent with the expected temperature value at the center of the laser-irradiated spot area, i.e. ~65 °C (see Fig. 1), which has been previously shown to represent the threshold value below which the fibrillar collagen keeps undenatured [17].

In order to quantify these observations, we carried out an FFT analysis of the polarization profiles, which are regarded as the superposition of three contributions, as explained before (see Sec. 2.4.2). In particular, we considered the distribution of the values of the noise-subtracted low frequency component normalized by the zero frequency component (*MP*). This parameter is readily accessible, proves sensitive to the local loss of anisotropy, and allows for the detection of even minor deviations from the normal reference profile. The limit value of zero represents the isotropic situation, and physically corresponds to the complete disorganization of the fibrillar distribution. Progressively higher values correspond to increasing degrees of order, i.e. of better alignment of the fibrils. Typical *MP* values extracted from the control areas are $MP = (6.85 \pm 0.10)$ %, which is taken as the highly ordered limit in the corneal stroma. In contrast, average values of $MP = (2.39 \pm 0.09)$ % (intermediate loss of anisotropy) are found in the laser-treated areas.

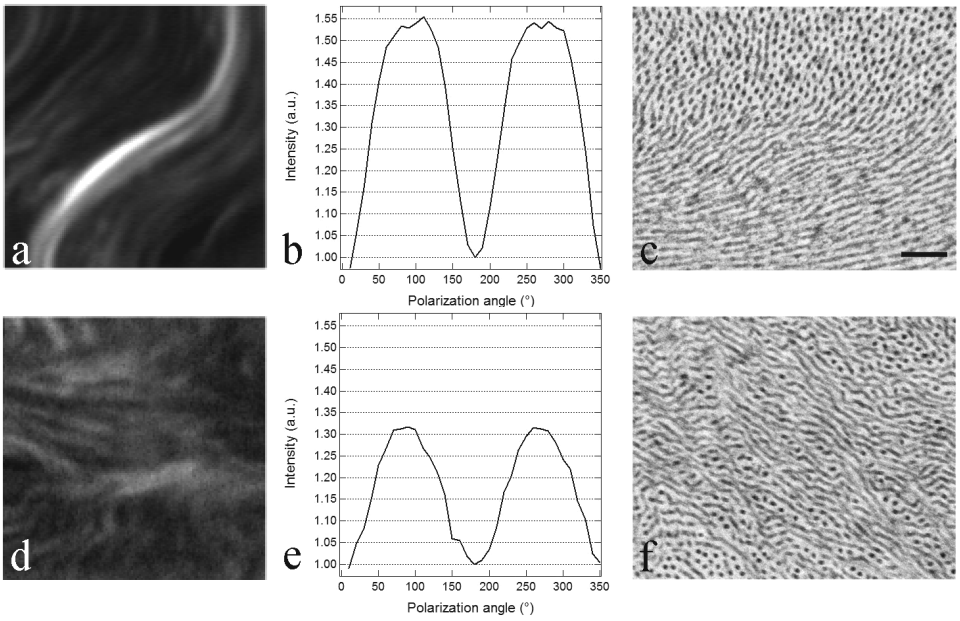

Fig. 7. Polarized-SHG and TEM analyses of the interfibrillar alignment. Left: SHG images (12×12 μm^2) of a control (a) and a laser-irradiated (d) region taken at a radial distance of 600 and 0 μm from the center of a laser-irradiated spot area, respectively. Middle: (b,e) average polarization profiles of single points (0.5 μm size, n = 1000) taken randomly from control (a) and laser-irradiated (d) regions, respectively. Right: TEM micrographs (bar = 300 nm) showing the nanometric assembly of collagen fibrils in a control (c) and laser-irradiated (f) region.

#103227 - $15.00 USD Received 24 Oct 2008; revised 26 Nov 2008; accepted 27 Nov 2008; published 13 Mar 2009

4. Conclusions

We have introduced an empirical approach based on three complementary analytical methods to process the SHG signals and characterize the corneal stroma disorganization induced by photothermal effects following laser irradiation. This disorganization was probed at different hierarchical levels of the collagen assembly. The lamellar disorder was effectively quantified by the variation of the 2D DFT magnitude and of the image entropy of circularly-polarized SHG images. We then took advantage of the polarization dependence of the SHG intensities to extract maps of the local orientation of the collagen fibrils. These maps were used to retrieve the typical distance over which the regular sub-lamellar arrangement is preserved when passing from the laser-untreated to the laser-treated areas. We finally probed the changes in the fibrillar packing at the sub-micron scale by a simple analysis of the modulation of the polarization profiles.

Similar analytical procedures may be applied to study several genetic, pathologic, accidental or surgical-induced disorder states of biological tissues. Moreover, on account of the emerging potential of SHG imaging to become an *in vivo* diagnostic tool, the proposed analytical methods may find future application in the clinical setting.

#103227 - $15.00 USD Received 24 Oct 2008; revised 26 Nov 2008; accepted 27 Nov 2008; published 13 Mar 2009